Journal of Solid State Chemistry **166,** 285–291 (2002)
doi:10.1006/jssc.2002.9586

Phase Equilibrium in the System Ln–M–O

III. Ln=Gd at 1100°C

Kenzo Kitayama,[1] Hiroyuki Ohno, Yusuke Ide, Keisuke Satoh, and Saori Murakami

Department of Applied Chemistry and Biotechnology, Faculty of Engineering, Niigata Institute of Technology, Kashiwazaki, Niigata 945-1195, Japan

Received November 16, 2001; in revised form March 4, 2002; accepted March 15, 2002

Phase equilibrium in the system Gd–Mn–O has been established at 1100°C while varying the partial pressure of oxygen between 0 and 13.00 in $-\log(P_{O_2}/\text{atm})$, and a phase diagram at 1100°C is presented as a Gd_2O_3–MnO–MnO_2 system. Under the experimental conditions, Gd_2O_3, MnO, Mn_3O_4, $GdMnO_3$, and $GdMn_2O_5$ phases are present at 1100°C, but Gd_2MnO_4, Mn_2O_3, and MnO_2 are not stable in the system. The substantial difference from the previously studied La–Mn–O and Nd–Mn–O systems lies in the fact that the $LnMn_2O_5$-type phase is stable under the present experimental conditions. A wide range of nonstoichiometry has been found in the $GdMnO_3$ phase coexisting with Gd_2O_3. X in $GdMnO_{3+X}$ ranges from -0.03 at $\log P_{O_2} = -9.47$ to 0.05 at $\log P_{O_2} = 0$. Nonstoichiometry is represented by an equation, $N_O/N_{GdMnO_3} = 3.00 \times 10^{-4}(\log P_{O_2})^3 + 5.80 \times 10^{-3}(\log P_{O_2})^2 + 3.52 \times 10^{-2}(\log P_{O_2}) + 0.0464$, and the activities of components in solid solution are calculated from the equation. Similar to the case of $LaMnO_3$, $GdMnO_3$ seems to vary in composition between the Gd_2O_3-rich and Gd_2O_3-poor sides. Lattice constants of $GdMnO_3$ produced under different oxygen partial pressures and those of $GdMn_2O_5$ prepared in air were determined, along with spacings and relative intensities of $GdMn_2O_5$. Standard Gibbs energies of reactions shown in the system were calculated and compared with previously reported values.

Key Words: **phase equilibrium; thermogravimetry; gadolinium-manganese oxide; standard Gibbs energy change of reaction.**

INTRODUCTION

Recently, phase equilibrium has been established in the Ln–Mn–O (*Ln* = La(1) and Nd(2)) systems at 1100°C. Only the $LnMnO_3$ type has been found stable under the experimental conditions as a ternary compound. An $LnMn_2O_5$ phase has not been found, although this phase is stable in the *Ln*–Mn–O system (3–7).

As has been well known, four stable oxide phases exist in the Mn–O system: MnO, Mn_3O_4, Mn_2O_3, and MnO_2. However, only two oxide phases, MnO and Mn_3O_4, are stable under the experimental conditions (1, 2). The oxygen partial pressure in equilibrium with MnO and Mn_3O_4 has been found to be -5.40 in $\log(P_{O_2}/\text{atm})$.

Many reports have been published on $LaMnO_3$ from the view point of magnetic, electronic, and crystallographic properties (8–18). In contrast, not many reports have been published on other lanthanoid–manganese perovskites, although the same physical and chemical properties would be expected.

In a Gd–Mn–O system, $GdMnO_3$ and $GdMn_2O_5$ are stable ternary phases. Pyroelectric current measurement of a $GdMn_2O_5$ single crystal was performed between 4.2 and 273 K, and these results indicate the existence of spontaneous polarization at low temperature (19). Thermodynamic properties of $GdMn_2O_5$ was derived from measurements of enthalpy and heat capacity (6). $GdMn_2O_5$ was prepared by a wet method in which metallic Mn and Gd_2O_3 was dissolved into HNO_3, in view of the difficulty in inducing the usual solid reaction of manganese oxide and gadolinium oxide.

Phase equilibrium in the Gd–Mn–O system, which well represents the stability relations among the phases, has not been established even at high temperatures.

In consideration of the above circumstances, the objectives of the present study are (1) to establish a detailed phase diagram of the Gd–Mn–O system at 1100°C as a function of oxygen partial pressure and to ascertain the nonstoichiometric range of $GdMnO_3$ and $GdMn_2O_5$, (2) to determine the thermochemical properties from the established phase diagram, and (3) to determine the crystallographic properties of $GdMn_2O_5$ if it would be stable.

EXPERIMENTAL

Analytical grade Gd_2O_3 (99.9%) and MnO (99.9%) were used as starting materials. MnO was dried by heating at 110°C in air, and Gd_2O_3 was also dried at 1100°C.

[1] To whom correspondence should be addressed. Fax: +257-22-8142. E-mail: kitayama@acb.niit.ac.jp.

0022-4596/02 $35.00

Mixtures having desired ratios of Gd_2O_3/MnO were prepared by solid-state reaction through mixing in an agate mortar and then carrying out calcination repeatedly during the intermediate mixing. Subsequent steps were followed by the same procedures as described previously (20).

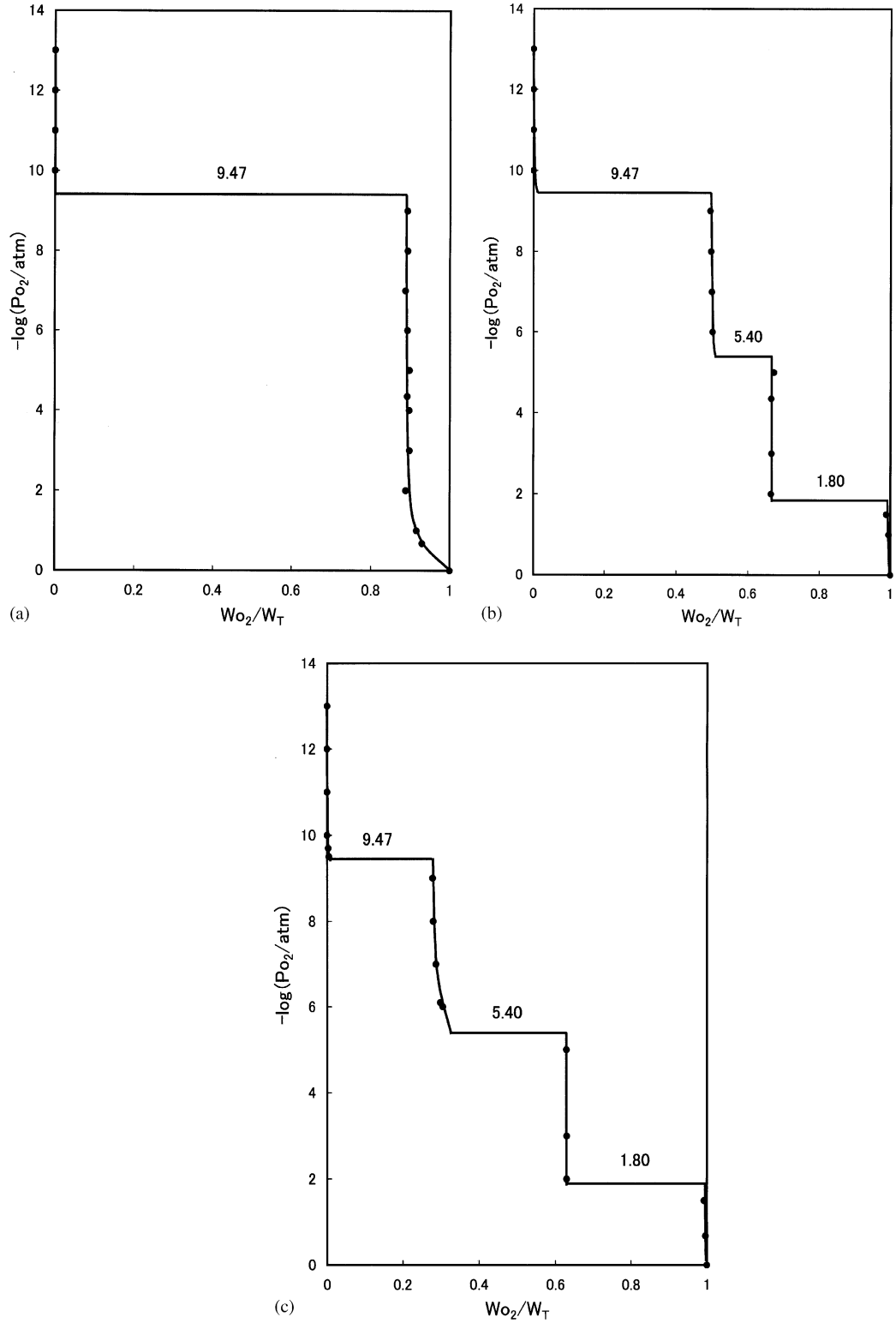

FIG. 1. Relationships between oxygen partial pressure, $\log(P_{O_2}/\text{atm})$, and weight change of the samples, W_{O_2}/W_T : (a) Gd_2O_3/MnO = 0.40/0.60; (b) Gd_2O_3/MnO = 0.25/0.75; and (c) Gd_2O_3/MnO = 0.15/0.85.

TABLE 1
Identification of Phase

Sample Gd_2O_3/MnO	$-\log P_{O_2}$ (atm)	Time (h)	Phase
0.6/0.4	13	8	$Gd_2O_3 + MnO$
	10	8	$Gd_2O_3 + MnO$
	9	17	$Gd_2O_3 + GdMnO_3$
	0.68	20	$Gd_2O_3 + GdMnO_3$
0.4/0.6	13	8	$Gd_2O_3 + MnO$
	10	8	$Gd_2O_3 + MnO$
	9	17	$Gd_2O_3 + GdMnO_3$
	0.68	20	$Gd_2O_3 + GdMnO_3$
0.25/0.75	13	8	$Gd_2O_3 + MnO$
	10	8	$Gd_2O_3 + MnO$
	9	17	$GdMnO_3 + MnO$
	6.5	21.5	$GdMnO_3 + MnO$
	5	24.5	$GdMnO_3 + Mn_3O_4$
	0.68	96	$GdMnO_3 + GdMn_2O_5$
0.15/0.85	13	8	$Gd_2O_3 + MnO$
	10	8	$Gd_2O_3 + MnO$
	9	17	$GdMnO_3 + MnO$
	6.5	21.5	$GdMnO_3 + MnO$
	5	24.5	$GdMnO_3 + Mn_3O_4$
	0.68	96	$GdMn_2O_5 + Mn_3O_4$

In the present experiment, oxygen partial pressure was obtained by use of a mixed gas of CO_2 and H_2 and 1 atm of O_2, and a mixed gas of CO_2 and O_2, and 1 atm of CO_2.

The apparatus and procedures for controlling oxygen partial pressure and maintaining constant temperature, the method of thermogravimetry, and the criterion for the establishment of equilibrium were the same as those described in our previous paper (20). The method of establishing equilibrium can be briefly described as follows. To ensure equilibrium, the equilibrated point of each sample at a given oxygen partial pressure was determined from both sides of the reaction, that is, from low oxygen partial pressure to high oxygen partial pressure and vice versa. The balance, furnace, and gas mixer are schematically shown in (21). The furnace is installed vertically and employs as its heating element a mullite tube wound with Pt 60%–Rh 40% alloy wire. Mixed gases, which ensure the desired oxygen partial pressures are passed from the bottom of the furnace to the top.

Identification of phases and determination of lattice constants were performed with a Rigaku X-ray diffractometer, model Rint 2500, employing Ni-filtered Cu$K\alpha$ radiation. A specimen of silicon was used to calibrate 2θ as an external standard.

RESULTS AND DISCUSSION

Gd_2O_3–MnO–MnO_2 System

The Mn–O system at 1100°C related to the present phase diagram has been described in previous studies (1, 2). Here, the results are briefly described as follows: the MnO and Mn_3O_4 phases are stable, and MnO is nonstoichiometric,

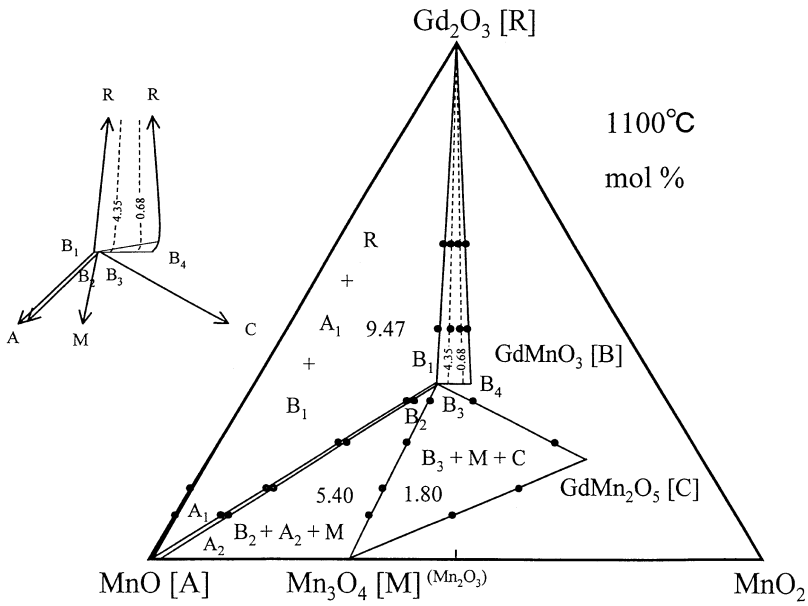

FIG. 2. Phase equilibrium in the Gd_2O_3–MnO–MnO_2 system at 1100°C. Numerical values in the three-phase regions represent oxygen partial pressures in $-\log(P_{O_2}(\text{atm}))$ in equilibrium with three solid phases, which are shown in the regions. Dotted lines in the two-phase regions also represent oxygen partial pressures indicated on the lines. Abbreviations are the same as those used in Table 2.

TABLE 2
Compositions, Symbols, Oxygen Partial Pressures in Equilibrium, and Activities of Components in Solid Solutions

Component	Compositions	Symbols	$-\log P_{O_2}$ (atm)	$\log a_i$
MnO	$MnO_{1.00}$	A	13.00–10.00	0
	$MnO_{1.00}$	A_1	9.47	5.62×10^{-4}
	$MnO_{1.03}$	A_2	5.40	-9.6×10^{-3}
$GdMnO_3$	$GdMnO_{2.97}$	B_1	9.47	0
	$GdMnO_{2.98}$	B_2	5.40	0.0391
	$GdMnO_{2.99}$	B_3	1.80	0.0686
	$GdMnO_{3.05}$	B_4	0	0.0501

whereas Mn_3O_4 is stoichiometric. The oxygen partial pressure in equilibrium with MnO and Mn_3O_4 is -5.40 in $\log(P_{O_2}/\text{atm})$.

Six samples, having Gd_2O_8/MnO mole ratios of 0.6/0.4, 0.4/0.6, 0.3/0.7, 0.25/0.75, 0.15/0.85, and 0.1/0.9, were prepared for thermogravimetry. Figure 1 shows for three representative samples: 0.4/0.6 (Fig. 1a), 0.25/0.75 (Fig. 1b), and 0.15/0.85 (Fig. 1c), the oxygen partial pressure, $-\log(P_{O_2}/\text{atm})$, versus weight change, W_{O_2}/W_T. Here, W_{O_2} is the weight increase of a sample from the reference weight at $\log(P_{O_2}/\text{atm}) = -13.00$, at which Gd_2O_3 and MnO are stable, and W_T is the total weight gain from the reference state to the state at 1 atm O_2, at which Gd_2O_3 and $GdMnO_3$, $GdMnO_3$ and $GdMn_2O_5$, or $GdMn_2O_5$ and Mn_3O_4 are stable, depending on the overall composition of the sample. As is evident from Fig. 1, weight breaks are found at 9.47, 5.40, and 1.80 in $-\log(P_{O_2}/\text{atm})$. These values correspond to the oxygen partial pressure in equilibrium with three solid phases, $Gd_2O_3 + GdMnO_3 + MnO$, $GdMnO_3 + MnO + Mn_3O_4$, or $GdMnO_3 + Mn_3O_4 + GdMn_2O_5$, respectively.

Table 1 shows the results of identifying phases in the Gd–Mn–O system, together with the experimental conditions. Samples of about 500 mg were produced for the identification of phases, by means of the quenching method. Five phases, Gd_2O_3, MnO, Mn_3O_4, $GdMnO_3$, and $GdMn_2O_5$, were found to be stable under the experimental conditions.

From the above results of thermogravimetry and the phase identification, a phase diagram was drawn. The phase diagram is shown in Fig. 2 as a Gd_2O_3–MnO–MnO_2 system, although MnO_2 is not stable under the experimental conditions. The numerical values in the three solid fields in Fig. 2 are values in $-\log P_{O_2}$ in equilibrium with the three solid phases described above, and those found in the two-phase regions are also oxygen partial pressures in $\log P_{O_2}$, which are shown by dotted lines. Table 2 lists the compositions, symbols, stability ranges in the oxygen partial pressures of compound, and activities of components in the solid solutions. Nonstoichiometry of MnO is ascertained by the results of thermogravimetry of the other two samples, shown in Figs. 1b and 1c. That is, nonstoichiometry is represented by slight changes in composition within the oxygen partial pressure range of 9.47–5.40 in $-\log P_{O_2}$.

$GdMnO_3$ has a large nonstoichiometric composition region with in the range of -9.47–0 in $\log P_{O_2}$. Figure 3 shows the relationship between oxygen partial pressure and composition of the $GdMnO_3$ solid solution, which coexisted with Gd_2O_2. This curve is represented by an equation: $N_O/N_{GdMnO_3} = 3.00 \times 10^{-4}(\log P_{O_2})^3 + 5.80 \times 10^{-3}(\log P_{O_2})^2 + 3.52 \times 10^{-2}(\log P_{O_2}) + 0.0464$. Here, N_O and N_{GdMnO_3} represent the mole fraction of oxygen and $GdMnO_3$ in the solid solution. This equation can be solved to show that gadolinium–manganese perovskite would be stoichiometric at -1.79 in $\log(P_{O_2}/\text{atm})$. As shown in

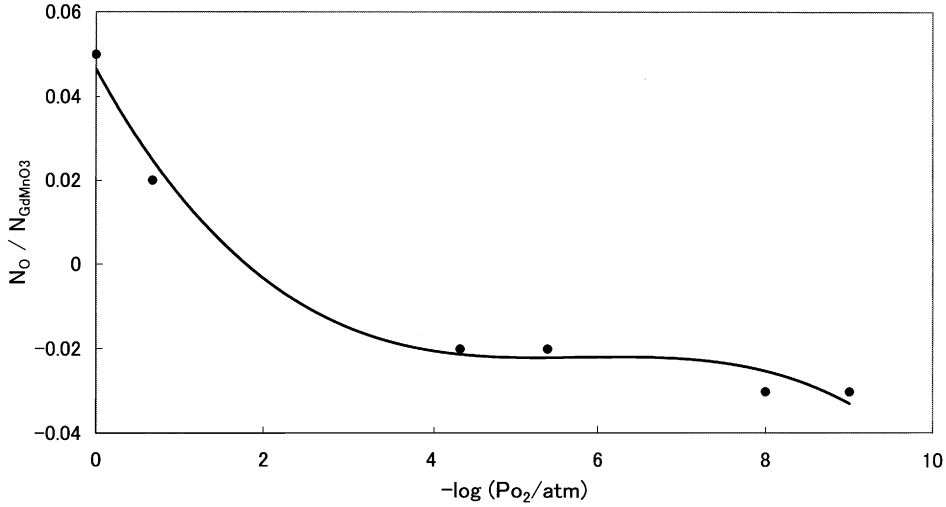

FIG. 3. Oxygen partial pressure, $-\log(P_{O_2}/\text{atm})$ versus the composition of $GdMnO_3$ solid solution. N_O/N_{GdMnO_3}.

TABLE 3
Lattice Contents of Quenched $GdMnO_3$

Sample Gd_2O_3/MnO	Phases coexisted	$-\log P_{O_2}$ (atm)	a (Å)	b (Å)	c (Å)	V (Å^3)
0.6/0.4	Gd_2O_3	9.00	5.315(2)	5.862(4)	7.426(2)	231.3(2)
	Gd_2O_3	0.68	5.311(6)	5.842(10)	7.425(5)	230.4(5)
0.4/0.6	Gd_2O_3	9.00	5.316(3)	5.840(5)	7.433(4)	230.8(3)
	Gd_2O_3	0.68	5.322(8)	5.807(9)	7.433(8)	229.7(5)
0.25/0.75	MnO	9.00	5.313(2)	5.847(3)	7.431(2)	230.9(1)
	MnO	6.50	5.313(2)	5.837(3)	7.425(2)	230.3(1)
	Mn_3O_4	5.00	5.308(4)	5.825(5)	7.425(4)	229.6(3)
	$GdMn_2O_5$	0.68	5.316(8)	5.847(5)	7.433(7)	231.0(5)
0.15/0.85	MnO	9.00	5.314(2)	5.843(3)	7.428(3)	230.7(2)
	MnO	6.50	5.312(2)	5.841(4)	7.425(2)	230.3(2)
	Mn_3O_4	5.00	5.308(6)	5.853(9)	7.425(7)	230.7(5)
JCPDS Card No. 25–337 Ref. (27)			5.310	5.840	7.430	
Ref. (28)			5.338	5.879	7.450	
Ref. (29)			5.316	5.856	7.434	

Fig. 2, the composition of the $GdMnO_3$ solid solutions on the Gd_2O_3-rich side and that on Gd_2O_3-poor side are not the same. This suggests that the region exhibits some width with respect to the direction between the Gd_2O_3 side and the Mn_3O_4 side. Van Roosmalen *et al.* (18) reported that a perovskite-type $LaMnO_{3+\delta}$ solid solution can be formed with excess La as well as with excess Mn. The same phenomenon was also found in relation to the La–Mn–O (6) and Nd–Mn–O (7) systems. A tentative detailed, enlarged inset of the $GdMnO_3$ region is drawn in the upper left-hand side of Fig. 2 in an exaggerated manner. However, its width has not been detected by the present experimental techniques. The curved lines of $\log P_{O_2}$ are drawn from the Gibbs phase rule, that is, one-phase region of three-component system has two degrees of freedom.

TABLE 4
Standard Gibbs Energy Changes of Reaction at 1100°C

Reaction	$-\log P_{O_2}$ (atm)	$-\Delta G^0$ (kJ/mol)
(1) $3MnO + 1/2O_2 \rightarrow Mn_3O_4$	5.40	72.1
	5.62	73.9[a]
		60.4[b]
		50.9[c]
(2) $1/2Gd_2O_3 + MnO + 1/4O_2 \rightarrow GdMnO_3$	9.47	62.2
	9.36	61.5[d]
(3) $GdMnO_3 + 1/3Mn_3O_4 + 1/3O_2 \rightarrow GdMn_2O_5$	1.80	14.0
	1.95	15.3[e]

[a] Ref. (23).
[b] Ref. (24).
[c] Ref. (25).
[d] Ref. (26).
[e] Ref. (27).

Consequently, the oxygen partial pressure lines in the one-phase area, the $GdMnO_3$ phase, could be curved.

Lattice constants of $GdMnO_3$ perovskite were determined as orthorhombic at 9.00, 6.50, 5.00, and 0.68 in $-\log P_{O_2}$ from samples of Gd_2O_3/MnO at mole ratios of 0.6/0.4, 0.4/0.6, 0.25/0.75, and 0.15/0.85. These samples were selected from their ability to coexist with Gd_2O_3, MnO, Mn_3O_4, and $GdMn_2O_5$, respectively. The results are tabulated in Table 3, together with the previously reported values. Significant differences were found in the lattice constants and the volumes of these samples, depending on the oxygen partial pressure in the case of coexistence with Gd_2O_3. The samples prepared in 0.68 in $-\log P_{O_2}$ are of smaller volume than those prepared at 9.00 in $-\log P_{O_2}$. This could stem from the difference in the ionic radii, that is, Mn^{3+} has an ionic radius of 0.72 Å and Mn^{4+} an ionic radius of 0.68 Å, with each having a coordination number of 6 (22). Meanwhile, the differences in lattice constants and volume between samples of 0.25/0.75 and 0.15/0.85 were within experimental errors. This is reasonable from Fig. 2, in which compositions of $GdMnO_3$ fall with in small ranges.

Standard Gibbs Energy Change of Reaction

On the basis of the established phase diagram, the standard Gibbs energy changes of reactions in Table 4 were determined by the equation, $\Delta G^\circ = -RT \ln K$. Here, R is the gas constant, T the absolute temperature, and K the equilibrium constant of the reaction. The standard state of activities of components in the solid solutions can be

TABLE 5
Lattice Constant of Quenched $GdMn_2O_5$

Sample Gd_2O_3/MnO	$-\log P_{O_2}$ (atm)	a (Å)	b (Å)	c (Å)	V (Å^3)
0.2/0.8	0.68	7.293(5)	8.542(6)	5.687(3)	354.3(4)
Ref. (4)		7.36	8.52	5.69	356.8
Ref. (6)		7.337	8.536	5.683	357

arbitrarily chosen for each solid solution, and in Table 2 the standard state is indicated as $\log a_i = 0$.

The previously reported values of ΔG° and the oxygen partial pressure in equilibrium with MnO and Mn_3O_4 are quoted from Refs. (23–25). The standard Gibbs energy change for reaction (1) is -72.1 ± 0.4 kJ/mol. Taking the activity of MnO of the composition (A_2) as unity, this value is -75.0 ± 0.3 kJ/mol. This difference is larger than an experimental error. It shows that the calculation of activity in solid solution is necessary. Calculating from the previous data of (23–25) yields -73.9, -60.4, and -50.9 kJ/mol, respectively.

The ΔG° value for reaction (2) is -62.2 kJ/mol, and this value shows fairly close agreement with -61.5 kJ/mol (26). The present value is larger than those of -85.3 for $LaMnO_3$, and -71.3 for $NdMnO_3$, as would be expected from the higher oxygen partial pressure in equilibrium.

The oxygen partial pressure in equilibrium and ΔG° value for reaction (3) are -1.80 ± 0.05 in $\log(P_{O_2}/\text{atm})$ and -14.0 kJ/mol. These values show close agreement with the previously reported values, -1.95 and -15.3 (4), respectively.

Compound, $GdMn_2O_5$

Unlike the La and Nd systems, in the Gd–Mn–O system $GdMn_2O_5$ is stable as a ternary compound. Preparing the compound by solid reaction of a mixture of gadolinium and manganese oxide is time consuming even at 1100°C, on account of the slow reaction rate. Producing $GdMn_2O_5$ in air takes more than 2 days.

The compound might be stoichiometric. Lattice constants and spacings were determined from the data of $DyMn_2O_5$ (27). Determined lattice constants are shown in Table 5 together with previously reported values. The spacings and relative intensities are shown in Table 6. The density of $GdMn_2O_5$ produced in air was determined to be 6.49 g/cm^3, by the usual pycnometric method. This value shows close agreement with 6.46 g/cm^3 reported by Bertaut *et al.* (4). From the obtained volume of a unit cell, Z is calculated as 3.99. Z must be an integer, and would be 4. This number corresponds to that of $DyMn_2O_5$(5).

CONCLUSIONS

(1) Phase equilibrium in the system Gd–Mn–O at 1100°C was established under an oxygen partial pressure ranging from 0 to -13.00 in $\log(P_{O_2}/\text{atm})$.

(2) Under the present experimental conditions, the Gd_2O_3, MnO, Mn_3O_4, $GdMnO_3$, and $GdMn_2O_5$ phases are stable.

(3) MnO and $GdMnO_3$ have nonstoichiometric compositions. However, Mn_3O_4, and $GdMn_2O_5$ are stoichiometric.

TABLE 6
Spacing and Relative Intensities of $GdMn_2O_5$

h	k	l	d(obs.)	d(cal.)	$I/I_0 \times 100$
1	2	0	3.690	3.686	15
0	2	1	3.416	3.415	10
1	2	1	3.099	3.093	66
2	1	1	2.906	2.889	100
0	0	2	2.843	2.844	13
2	2	0	2.788	2.773	6
1	3	0	2.657	2.650	38
1	1	2	2.533	2.530	27
1	3	1	2.407	2.404	6
0	2	2	2.366	2.367	19
1	2	2	2.250	2.251	12
2	1	2	2.176	2.169	33
1	4	0	2.051	2.049	13
2	2	2	1.991	1.985	26
1	4	1	1.930	1.928	21
0	0	3	1.895	1.896	4
3	3	0	1.859	1.849	5
2	4	0	1.840	1.843	6
1	1	3	1.799	1.794	6
3	3	1	1.766	1.758	15
0	4	2	1.707	1.708	17
1	2	3	1.687	1.686	18
1	5	0	1.664	1.663	6
2	1	3	1.653	1.650	21
1	5	1	1.596	1.597	2
3	3	2	1.555	1.550	23
4	0	2	1.545	1.535	18
4	1	2	1.520	1.511	3
2	5	1	1.495	1.493	13
3	1	3	1.477	1.473	1
2	3	3	1.451	1.448	2
5	1	0	1.436	1.438	7
0	0	4	1.422	1.422	15
3	5	0	1.402	1.398	4
1	4	3	1.392	1.392	12
5	2	0	1.381	1.380	2
1	6	1	1.361	1.357	4
4	3	2	1.352	1.351	4
1	2	4	1.327	1.326	8
2	1	4	1.310	1.309	2
0	6	2	1.272	1.273	2
1	3	4	1.253	1.253	10
3	4	3	1.227	1.225	3
6	0	0	1.212	1.215	3

(4) Standard Gibbs energies of reactions found in the diagram were calculated from the oxygen partial pressure in equilibrium with three solid phases.

(5) Lattice constants of $GdMnO_3$ and $GdMn_2O_5$, and the spacing, relative intensity, and density of $GdMn_2O_5$ were determined.

ACKNOWLEDGMENTS

The authors express their sincere gratitude to The Uchida Energy Science Promotion Foundation for lending financial support.

REFERENCES

1. K. Kitayama, *J. Solid State Chem.* **153,** 336 (2000).
2. K. Kitayama and T. Kanzaki, *J. Solid State Chem.* **158,** 236 (2001).
3. S. Quezel-Ambrunaz, F. Bertaut, and G. Buisson, *C. R. Acad. Sci. Paris* **258,** 3025 (1964).
4. E. F. Bertaut, G. Buisson, A. Durif, J. Mareschal, M. C. Montmory, and S. Quezel-Ambrunaz, *Bull. Soc. Chim. Fr.* 1132 (1965).
5. S. C. Abrahams and J. L. Bernstein, *J. Chem. Phys.* **46,** 3776 (1967).
6. H. Satoh, S. Suzuki, K. Yamamoto, and N. Kamegashira, *J. Alloys Compd.* **234,** 1 (1996).
7. J. A. Alonso, M. T. Casais, M. J. Martinez-Lope, J. L. Martinez, and M. T. Fernandez-Diaz, *J. Phys.: Condens. Matter* **9,** 8515 (1997).
8. J. B. Goodenough, *Prog. Solid State Chem.* **5,** 149 (1971).
9. C. N. R. Rao, *Annu. Rev. Phys. Chem.* **40,** 291 (1989).
10. B. C. Tofield and W. R. Scott, *J. Solid State Chem.* **10,** 183 (1974).
11. F. Abbattista and M. Lucco Borlera, *Ceram. Int.* **7**(4), 137 (1981).
12. G. Matsumoto, *J. Phys. Soc. Jpn.* **29,** 606 (1970).
13. J. H. Kuo and H. U. Anderson, *J. Solid State Chem.* **83,** 52 (1989).
14. B. C. Hauback, H. Fjellvag, and N. Sakai, *J. Solid State Chem.* **124,** 43 (1996).
15. K. Kamata, T. Nakajima, T. Hayashi, and T. Nakamura, *Mater. Res. Bull.* **13,** 49 (1978).
16. T. Nakamura, G. Petzow, and L. J. Gauckler, *Mater. Res. Bull.* **14,** 649 (1979).
17. M. Lucco Borlera and F. Abbattista, *J. Less-common Metals* **92,** 55 (1983).
18. J. A. M. van Roosmalen, P. van Vlaanderen, E. H. P. Cordfunke, W. L. Ijdo, and D. J. W. Ijdo, *J. Solid State Chem.* **114,** 516 (1995).
19. A. Inomata and K. Kahn, *J. Phys. Condens. Matter* **8,** 2673 (1996).
20. K. Kitayama, K. Nojiri, T. Sugihara, and T. Katsura, *J. Solid State Chem.* **56,** 1 (1985).
21. K. Kitayama, *J. Solid State Chem.* **137,** 255 (1998).
22. R. D. Shannon and C. T. Prewitt, *Acta Crystallogr. B* **25,** 925 (1965).
23. W. C. Hahn Jr. and A. Muan, *Am. J. Sci.* **258,** 66 (1960).
24. R. A. Robie, R. S. Hemingway, and J. R. Fisher, "Thermodynamic Properties of Minerals and Related Substances at 298.15 K and 1 Bar (10^5 Pascals) Pressure and at Higher Temperatures, Geological Survey Bulletin, No. 1452." United States Government Printing Office, Washington, 1978.
25. J. F. Elliott and M. Gleiser, "Thermochemistry for Steelmaking," Vol. 1. Addison-Wesley, Reading, MA, 1960.
26. T. Atsumi, T. Ohgushi, and N. Kamegashira, *J. Alloys Compd.* **238,** 35 (1996).
27. JCPDS Card No. 72-1696.
28. A. Waintal, J. J. Capponi, E. F. Bertaut, M. Contre, and D. Francois, *Solid State Commun.* **4,** 125 (1966).
29. G. J. McCarthy, P. V. Gallagher, and P. Sipe, *Mater. Res. Bull.* **8,** 1277 (1973).